On-line estimation of fuel consumption for producing electrical power in a vehicle

Sijs, J.

Award date:
2006

Eindhoven University of Technology
Department of Electrical Engineering
Control Systems

On-line estimation of fuel consumption for producing electrical power in a vehicle

by

Joris Sijs

Confidential

Master of Science thesis

Project period: February 2006
Report Number: 06A/02
Commissioned by: Prof.dr.ir. P.P.J. van den Bosch

Additional Commission members:
Dr. S. Weiland (TU/e)
Ir. J.T.B.A. Kessels (TU/e)
N.P.I. Aneke (FORD)

On-line estimation of fuel consumption for producing electrical power in a vehicle

Abstract

This paper describes a method to estimate on-line the additional costs for producing electrical power in a vehicle. The alternator power is excited with a small excitation signal of zero mean *dP*. In a feedback-loop the fuel-injection is excited with a similar signal with amplitude *df*. This amplitude is controlled with help of the correlation between the engine speed and the excitation on the alternator power *dP*. The aim of *df* is to compensate *dP*. The correlation determines whether *dP* is exactly compensated by *df* or not. The amplitude-ratio between *dP* and *df* provides the Incremental Fuel Rate (IFR=λ=*df/dP*). This quantity represents the derivative of the joint engine and the alternator map in an operating point. The method is designed and analysed on its stability and noise influence, which are verified with simulations.

1. Introduction

Due to the growing amount of electrical systems placed in a vehicle, the electrical energy consumption increases. Therefore, generating electrical power has become important because it directly influences the vehicle's fuel consumption. This fuel consumption is minimised with the help of energy management strategies, which use information of the vehicle's surrounding to choose an appropriate strategy. The aim is to give online information about the fuel consumption that is needed for the production of electrical energy. For that, the Incremental Fuel Rate (IFR) λ is determined, which is the additional fuel mass flow rate *df* [g/s] for producing a small amount of additional electrical power *dP* [W]. This paper describes a possible implementation for estimating this parameter online without affecting the drivability of the vehicle. First, the concept behind the identification method is shown in Section 2. Next, Section 3 explains the vehicle model that will be used to design the rest of the system, which is described in Section 4. A model for this identification system is derived in Section 5. The system is analysed on its stability, speed of convergence and noise influence in Section 6, 7 and 8 respectively. Finally in Section 9 simulations of the system are done and in Section 10 conclusions are drawn.

2. System description

The IFR combines information from the engine's fuel map and the alternator's efficiency. It makes sense to estimate λ [g/J] from the correlation between the fuel-injection f [g/s] and the generated alternator power P [W]. The engine's speed v [rad/s] is used to retrieve information about the response of the vehicle to f and P. The system for estimating λ, shown in Figure 1, consists of the vehicle itself, a system to calculate the correlation between v and dP (Corr.) and a controller (C) to calculate λ .

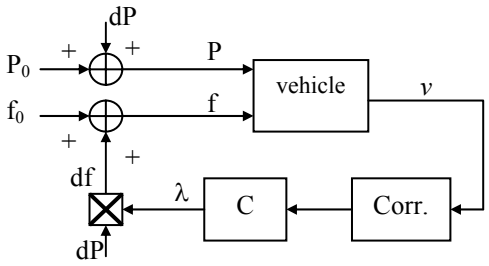

Figure 1: System description

The variables P_0 and f_0 are nominal input signals of the alternator power and fuel injection respectively and determine the point of operation of both the generator and the engine. The values of P and f must not become negative due to dP and df. The basic principle in estimating λ is to add a small signal dP to P_0 and compensate that by adding this same signal with the appropriate amplitude to f_0. The response of the vehicle to dP can be observed in the engine speed. This way, there is a correlation between dP and v. The fuel injection is excited with df, which equals dP multiplied with some constant λ. As long that there is a correlation between dP and the engine's speed, df does not compensate dP exactly and λ is adjusted. But when there is no effect visible on v, the ratio $\lambda=df/dP$, is the Incremental Fuel Rate. This parameter represents the additional fuel mass flow to produce 1 [W] additional electrical power without affecting the drivabilty. Notice that it is also possible to choose df as excitation and dP as feedback. The controller's output is in that case $1/\lambda$.

3. Vehicle model

Power is needed to drive a vehicle. The alternator turns mechanical power P_A into electrical power P, $P_A = \eta_A P$, with η_A the inverse efficiency. The relation between fuel-rate input f and fuel power P_f is: $P_f = \eta_f H_f f$. With η_f, the engine's efficiency and H_f [J/g] the Lower Heating Value of fuel. Air- and roll-friction must not be forgotten. Stalnaker [1] provides the relation between friction power and engine speed. All these powers together result in a total power used for acceleration. The relation between power and engine speed is denoted by:

$$\sum \frac{P}{v} = J\dot{v} \qquad (1)$$

With J the equivalent inertia of the vehicle seen at the engine. The model of a vehicle is shown in Figure 2.

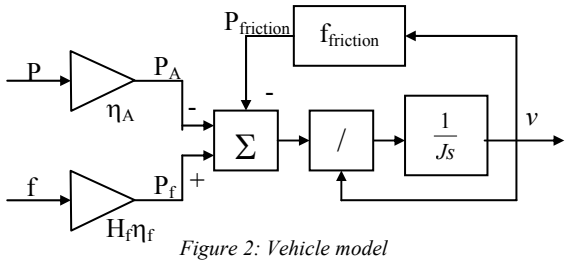

Figure 2: Vehicle model

4. Identification algorithm

Based on the vehicle model, the other parts of the system are designed. The steps that are considered here, are the excitation signal dP, the correlation-method, the controller and multiplying the controller's output with dP. All these parts together form the identification algorithm of λ.

a. Excitation signal

The design is started with the excitation signal dP. The crucial element of this signal is that it has zero mean so that P_0 is not influenced. Of all possible signals, three are the most interesting:

- Sinusoidal (sine)
- Square
- Pulse Width Modulation (PWM)

Note that the square is a special kind of PWM. The vehicle model has two inputs, P and f. One of them is used as primary-input, the other one as feedback-input. However, it has to be ensured that the feedback-input is capable of compensating the primary-input. In reality the alternator will be the first one that is bounded by its power limitations and therefore the electrical input P is used as primary-input.

The decision between sine or PWM is based on which one of them has the highest possible amplitude for the fundamental frequency. Given the nominal electrical power P_0 and the maximum power of the generator P_{max}, the maximum amplitude of the sine equals $a_{max} = \min(P_0, P_{max}-P_0)$. The PWM is able to switch between P_{max} and 0 with a period of T_f. The duty cycle D, to get a zero mean PWM, is:

$$D = \frac{P_0}{P_{\max}} \qquad (2)$$

Figure 3 shows a_{max} and the PWM ($=P-P_0$) in one plot.

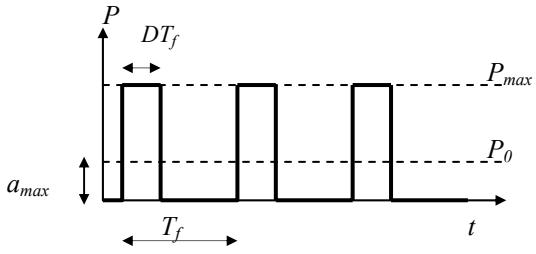

Figure 3: PWM signal (dP)

The PWM consists of an infinite number of harmonics for which each of them has a different amplitude and phase. This can be represented with a Fourier-series [2].

$$PWM = \frac{P_{\max}}{2}\sum_{n=1}^{\infty} a_n \cos\left(\frac{2n\pi}{T_f}t\right) + b_n \sin\left(\frac{2n\pi}{T_f}t\right) \qquad (3)$$

with:

$$a_n = \frac{2}{n\pi}\sin(2n\pi D)$$

$$b_n = \frac{2}{n\pi}(1-\cos(2n\pi D))$$

The amplitude of the sine (a_{max}) and of the fundamental of the PWM (frequency $\omega_f = 2\pi/T_f$ [rad/s]) are plotted against the duty cycle in Figure 4. Both plots have to be multiplied with P_{max} to come to their real value. It shows that the PWM amplitude always yields the largest amplitude at ω_f and thus will be used as input signal.

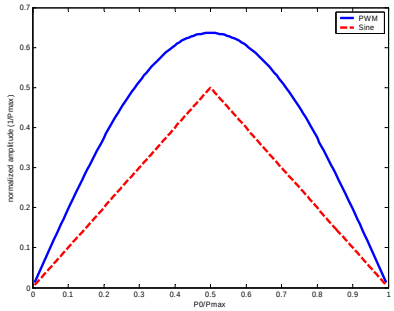

Figure 4: PWM (solid) versus sine (dashed)

b. Correlation and Controller

The correlation (Corr) and the controller (C) in Figure 1 are closely related to each other. In fact they can be seen as one big controller, but for clarity they are discussed separately.

The purpose of the correlation-block is to determine the amplitude of the disturbance in the engine speed as a response to dP and df.

The purpose of the controller-block is to calculate a λ that cancels the excitation of dP on the engine's speed.

Correlation is based on the multiplication of two signals. When two sinusoidal signals are multiplied, their product is:

$$\sin(\omega_1 t)\sin(\omega_2 t+\varphi) = \frac{1}{2}(\cos((\omega_1-\omega_2)t-\varphi)-\cos((\omega_1+\omega_2)t+\varphi)) \qquad (4)$$

The correlation element is that when an arbitrary signal u is multiplied with a sinusoidal signal with ω_f as frequency, their product will only have a DC-component if u contains the frequency ω_f.

Assuming that the vehicle behaves like an integrator for dP, it can be shown that it has the largest response to the fundamental frequency of dP. Thus correlation with ω_f gives the most reliable information (= highest DC), although higher harmonics can also be used for correlation. As long as the output of the correlation has a DC, it is certain that the engine's speed contains ω_f and that dP is not exactly compensated by df. But before this

multiplication takes place, v is filtered. The correlation is done at a frequency ω_f, so the filter will be a band-pass filter around ω_f. This filter is able to remove the huge constant engine speed due to f_0 and decrease the noise outside the frequency-band of interest.

For stability reasons it is important that the sign of the amplitude of df is correct, otherwise dP is helped instead of compensated. The sign of dP and df are such chosen that dP has a negative effect on the engine's speed and df a positive one. Let's make the agreement that when only dP is excited, the output of the correlation has the same sign as the amplitude of dP. There is a problem with the phase-shift ϕ due to the vehicle and the filter. Suppose dP equals $A\sin(\omega_f t)$. Multiplying the speed's response with $\sin(\omega_f t)$ results in:

$$\left(AK\sin\left(\omega_f t+\varphi\right)\right)\sin\left(\omega_f t\right)=\frac{AK}{2}\left(\cos(\varphi)-\cos\left(2\omega_f t+\varphi\right)\right) \quad (5)$$

In (5) A cannot be distinguished from φ and the system can only see its total DC = $\frac{1}{2}AK\cos(\varphi)$. Notice that when $\varphi = \pm 90^0$, the DC will be 0 no matter what A in reality is. This means that the correlation will act as if dP has already been compensated even though this is not the case. Furthermore, when $\varphi = 180^0$ the output of the correlation indicates the wrong sign, a negative A instead of a positive, resulting that df will help dP instead of compensating it. Two solutions to this problem are shown in Figure 5.

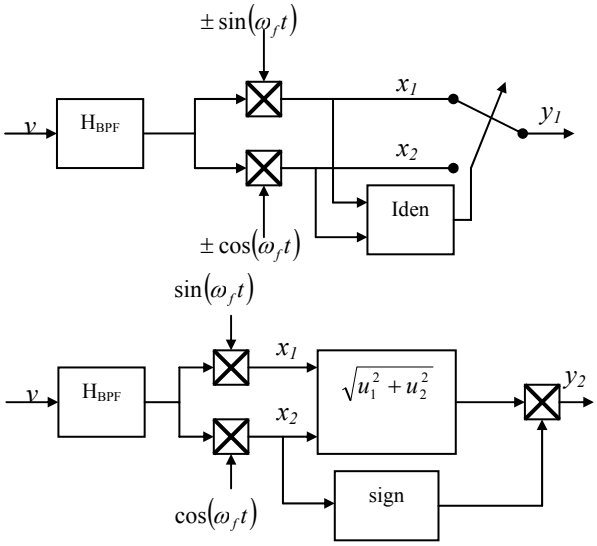

Figure 5: Two methods for correlation, upper system method 1, lower system method 2.

The choice between the two solutions depends on the expectation E of y_1 and y_2, the higher the better. If the filtered v contains $A\sin(\omega_f t+\varphi)$, then x_1 contains $^A/_2\cos\varphi$ and x_2 contains $^A/_2\sin\varphi$. But they also contain all other kinds of signals, which are all assigned to n. This n is assumed as a Gaussian noise function with zero mean and variance σ^2. The normalized expectations of both methods are calculated (independent of the amplitude A).

Expectation Method 1:

The identification-box chooses from x_1 and x_2 the signal with the highest DC and adds a minus sign to it if this DC, with df = 0, is negative. Suppose x_2 was chosen, then E is:

$$\frac{2}{A}E\left(x_2\right)=\frac{2}{A}E\left(n+\frac{A}{2}\sin\varphi\right)=\frac{2}{A}E(n)+\frac{2}{A}E\left(\frac{A}{2}\sin\varphi\right) \quad (6)$$
$$=\sin\varphi$$

If x_1 had been chosen, the outcome would be $\cos\varphi$. $E(y_1)$ is independent of noise and always between 1 and 0.7 (= $\sin 45^0 = \cos 45^0$) due to the identification-box.

Expectation Method 2:

$E\left(\sqrt{u_1^2+u_2^2}\right)$ is assumed to be $^A/_2$. This means that the normalized expectation of method 2 depends on the output of the sign-function. Suppose the input of the sign-function x_2 has the following properties:

$$P(x_2>0)=p;\quad P(x_2<0)=q=1-p \quad (7)$$

Then the normalized expectation of method 2 is:

$$E\left(sign\left(x_2\right)\right)=p-q=2p-1 \quad (8)$$

An example of x_2 ($x_2 = n+^A/_2\sin\varphi$), is shown in Figure 6.

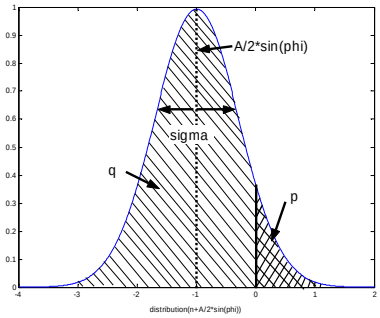

Figure 6: Distribution input sign-function

Figure 6 indicates that the expectation of method 2 is dependent on the amount of noise ($\sim\sigma^2$) and $^A/_2\sin\varphi$. Moreover, in the situation $\varphi = k180^0$, E = 0. But also when $^A/_2\sin\varphi$ is at its maximum but the noise is huge, the expectation of Method 2 is small. In formula we see:

$$E\left(y_2\right)_{\lim\sigma\to\infty}=0$$

Notice that the noise does not have to be Gaussian to have a small E. Any kind of noise with a large amplitude results in an expectation of almost zero. However, when there is little noise, the expectation can become 1 in all situations other then $\varphi = k180^0$.

In conclusion: Method 2 has a better performance for little noise and Method 1 is more robust. Because the noise in a vehicle is not known, a robust method is preferred and Method 1 is chosen as correlation method in this design.

Remark: The choice of a band-pass filter in front of the multiplication is not trivial. One could also use a low-pass filter after the multiplication. However, the band-pass filter is able to remove the constant engine speed c, which is about a 1000 times bigger then the response to dP. The multiplication shifts c towards a frequency of ω_f. Two drawbacks of the low-pass filter are:

- $H_{BPF}(0) = 0 << H_{LPF}(j\omega_f)$

- H_{LPF} has a larger settling-time than H_{BPF}.

The aim of the controller is to calculate λ such that the influence of *dP* is cancelled, thus that the input of the controller has no DC-component. Placing an integrator as controller together with a gain does this. The integrator is in equilibrium when its input has no DC, meaning that *dP* is exactly compensated by *df*. The influence of the gain is the speed of the convergence, the higher the gain the faster convergence.

c. Multiplication with dP

The output of the controller λ is multiplied with *dP* to get *df*. In case of exact compensation, the influence of *dP* on P_A is equal to the influence of *df* on P_f and λ can be calculated.

$$\eta_A dP = H_f \eta_f df = \lambda H_f \eta_f dP$$

$$\Rightarrow \lambda = \frac{\eta_A}{H_f \eta_f} \tag{9}$$

However, it is also possible to multiply λ with only the fundamental component of *dP*. With a_1 and b_1 from (3) the fundamental component of *dP* can be computed. The difference is that in this case the system will only compensate the fundamental of *dP* but (9) will remain the same. One thing should be kept in mind when λ is multiplied with the fundamental; the correlation should also be done with only the fundamental frequency. Otherwise the system will keep on finding a correlation between the engine's speed and one of the harmonics because those are not compensated.

In the multiplication with λ, *dP* is replaced by its fundamental sine-wave. Two benefits of this are:

- The signals in the system will not jump instantly but there is a smooth motion with an upper bound to the rate of change. It is known from plants with time-varying parameters that smoothly changing parameters may cause less instability than fast changing ones.
- The system will be easier to analyse and understand because parameters vary with one and the same frequency.

Now that the vehicle is modelled and the algorithm is designed, the closed-loop behaviour of the system is analysed. For that, a model of the system is made.

5. System model

Typically, the vehicle model expresses low-pass behaviour. The fundamental that goes into the vehicle will therefore get a phase-shift of -90^0. In that case the correlation-block will choose $\cos(\omega_f t)$ as multiplicand. The system of Figure 1 results in:

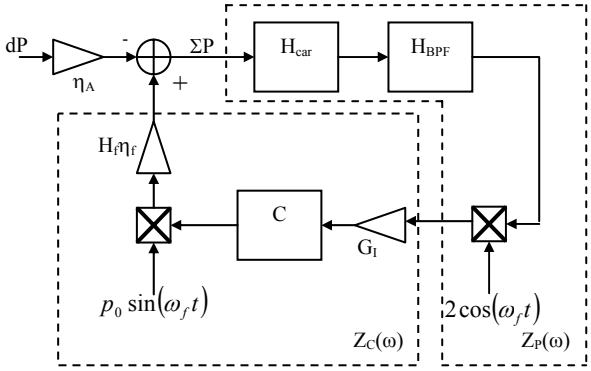

Figure 7: Identification system

In the system of Figure 7 it is assumed that the nominal friction power together with the nominal alternator power cancels the nominal fuel power. Thus only *dP* and *df* are left. The fundamental of *dP* is $p_0\sin(\omega_f t)$.
This system is converted into a model. This is explained in Appendix A. The following functions are defined:

$$Z_{P_n}(\omega) = H_{BPF}\left(j(\omega + n\omega_f)\right) H_{car}\left(j(\omega + n\omega_f)\right) \tag{10a}$$

$$Z_{C_n}(\omega) = G_I \frac{p_0 \eta_f H_f}{2} C\left(j(\omega + n\omega_f)\right) \tag{10b}$$

With n = 1,2,3… The model, shown in Figure 8, is divided into two parts, a signal generator and a function $Z(\omega)$.The signal generator produces all the harmonics of the input that are generated by the two multiplications. The function $Z(\omega)$ describes the effect of the input *r* and its harmonic on the output (ΣP in Figure 7).

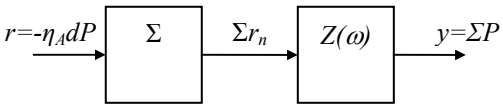

Figure 8: Model of the system

In the output of the signal generator r_n represents the harmonic with a frequency $\omega_0+n\omega_f$ with ω_0 the frequency of *r*. The function $Z(\omega)$ is a recursive combination of $Z_P(\omega)$, $Z_C(\omega)$ and the phase difference between the two sinusoidal multiplications ($\cos(\omega_f t)$ compared to $\sin(\omega_f t)$), which is 90^0 ($= e^{j\pi/2}$)):

$$Z(\omega) = \frac{1}{1 - Z_{P_0}\left(Z_-(\omega) + Z_+(\omega)\right)} \tag{11}$$

with

$$Z_-(\omega) = \frac{\left(e^{-j\frac{\pi}{2}} Z_{C_{-1}}(\omega)\right)}{1 - \left(e^{-j\frac{\pi}{2}} Z_{C_{-1}}(\omega)\right)\left(\frac{Z_{P_{-2}}(\omega)}{1 - Z_{P_{-2}}(\omega)(...)}\right)}$$

$$Z_+(\omega) = \frac{\left(e^{j\frac{\pi}{2}} Z_{C_{+1}}(\omega)\right)}{1 - \left(e^{j\frac{\pi}{2}} Z_{C_{+1}}(\omega)\right)\left(\frac{Z_{P_{+2}}(\omega)}{1 - Z_{P_{+2}}(\omega)(...)}\right)}$$

With the function of (11) the stability of the system can be analysed once all filters of (10) have been designed.

6. Stability analysis

Before analysing the stability the first question is what stability means for this system. Many signals in the system do not converge to some constant, but will always oscillate around some value. The best stability to be analysed is therefore BIBO-stability. Meaning that if the input is bounded, the output must also be bounded. Stability is analysed in two parts. In the first part, the model derived in Section 5 is analysed on its stability. In the second part other stability tests for dynamical systems are looked at. From now on it is assumed that the vehicle behaves like an integrator instead of a low-pass filter.

a. Stability of the linear model

To proof stability of the model, Σr_n has to be bounded and the function $Z(\omega)$ stable. First Nyquist-stability of $Z(\omega)$ is analysed. The filters of the system are:

$$H_{BPF}(j\omega) = \frac{aj\omega}{(j\omega)^2 + aj\omega + \omega_f^2} \tag{12a}$$

$$C(j\omega) = \frac{1}{j\omega} \tag{12b}$$

The parameter a determines the real part of the poles of the band-pass filter. When a is 0, the poles are on the imaginary axis, when a is ω_f, the poles are on the real axis. With (12), (10) results in:

$$Z_{P_n}(\omega) = \frac{a}{Jc}\frac{1}{\left(j(\omega + n\omega_f)\right)^2 + aj(\omega + n\omega_f) + \omega_f^2} \tag{13a}$$

$$e^{j\frac{\pi}{2}} Z_{C_n}(\omega) = G_I \frac{p_0 \eta_f H_f}{2}\frac{1}{(\omega + n\omega_f)} \tag{13b}$$

The analysis is simplified by assuming that all harmonics for which n is bigger then ±1 can be neglected because all filters are low-pass. This means that only signals born in the first loop are taken into account. Substituting the simplified version in (11):

$$Z(\omega) = \frac{1}{1 - Z_{P_0}(\omega)\left(\left(e^{j\frac{\pi}{2}} Z_{C_{+1}}(\omega)\right) + \left(e^{-j\frac{\pi}{2}} Z_{C_{-1}}(\omega)\right)\right)}$$

$$= \frac{1}{1 + G_I \frac{aH_f\eta_f p_0}{Jc}\frac{1}{(j\omega)^2 + a(j\omega) + \omega_f^2}\frac{\omega_f}{\omega^2 - \omega_f^2}} \tag{14}$$

The Nyquist-stability condition tells that the open loop function must never enclose the point –1 in the Nyquist-plot. At ω = 0 the denominator's value of (14) is negative-real. Thus the condition to guarantee stability of $Z(\omega)$ concerning the parameter G_I is:

$$G_I \frac{aH_f\eta_f p_0}{Jc}\frac{1}{\omega_f^3} < 1 \Rightarrow G_I < \frac{Jc\omega_f^3}{aH_f\eta_f p_0} \tag{15}$$

Σr_n is in this case already bounded because only r_{-1}, r_0 and r_{+1} are added to the input of $Z(\omega)$. Those signals are all bounded.

b. Stability of (non-linear) dynamical systems

There are a variety of stability methods for analysing the system of Figure 7, its differential equations are:

$$\begin{pmatrix} \dot{v} \\ \dot{x}_{BPF1} \\ \dot{x}_{BPF2} \\ \dot{\lambda} \end{pmatrix} = \begin{pmatrix} 0 & 0 & 0 & \frac{H_f\eta_f G_I p_0}{Jc}\sin(\omega_f t) \\ a & -a & -\omega_f^2 & 0 \\ 0 & 1 & 0 & 0 \\ 0 & 2\cos(\omega_f t) & 0 & 0 \end{pmatrix} \begin{pmatrix} v \\ x_{BPF1} \\ x_{BPF2} \\ \lambda \end{pmatrix} + \begin{pmatrix} -\eta_A \\ 0 \\ 0 \\ 0 \end{pmatrix} dP \tag{16}$$

The first method that is discussed uses a describing function [3]. This function gives a gain and phase for every frequency for a part of the system that cannot be described with a transfer function. In the case of the system in Figure 7 this part will be:

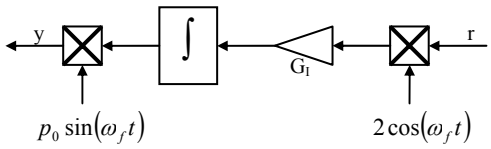

Figure 9: Elements covered with the describing function

When this part is fed with $\hat{r}\sin(\omega_0 t + \varphi)$, its output y, at frequency ω_0, is (see Appendix B):

$$y = -p_0 G_I \frac{\omega_f}{\omega_0^2 - \omega_f^2}\hat{r}\sin(\omega_0 t + \varphi) \tag{17}$$

The describing function $y = f(\omega)r$ of this part is:

$$f(\omega) = -p_0 G_I \frac{\omega_f}{\omega^2 - \omega_f^2} \tag{18}$$

With this description the system of Figure 7 becomes:

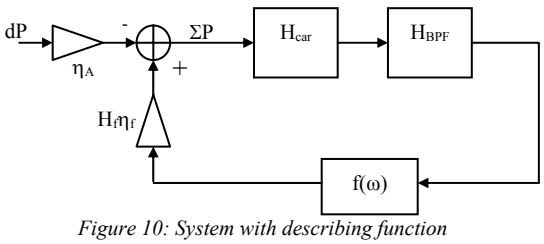

Figure 10: System with describing function

Notice that the transfer of the system in Figure 10 results in the same transfer as (14) and therefore leads to the same stability condition for G_I.

The second method utilizes a Linear Matrix Inequalities (LMI). Multiplication with a sinusoidal signal can be seen as a gain with a time-varying uncertainty and this can be analysed with an LMI. This method however could not find a stable region. The main reason for that is because this method analyses quadratic stability (if its input is zero, its output should 'quadraticly' go to zero). Due to the periodic signals in the system, this does not hold here.

The third method is known as 'averaging theory'. This theory uses the differential equations of (16):

$$\dot{x}(t) = \varepsilon f(t, x) \tag{19}$$

In this case $f(t,x)$ is periodic. The theory says that the system behaves according to the averaged version of (19) over one period:

$$\dot{x}(t) = \varepsilon f_{av}(x) \tag{20}$$

According to [4] and [5] two conditions are to be met. The first one is that the fluctuations due to the periodic coefficients should be slow compared to the dynamical

system surrounding it. The second one is that the oscillations should be small, as ε suggests. Both of them are not met. Further, $f_{av}(x)$ of (19) leads to the cancellation of the feedback, because Av(sin($\omega_f t+\varphi$))=0.

The fourth and last theory is the one from Poincaré and Floquet. There is an easier theory of Poincaré-Benedixson. However, this theory can only be used on 2D systems and (16) shows that the system is 4D. The theory of Floquet, [6] states that if there is a periodic system:

$$\dot{x} = A(t)x \tag{21}$$

Where $A(t)$ is an $n\times n$-matrix and T-periodic, every solution of the system has the same structure:

$$x(t) = P(t)e^{Bt} \tag{22}$$

Both $P(t)$ and B are an $n\times n$-matrix. The matrix $P(t)$ is T-periodic and describes a so called Poincaré-map. The B-matrix consists of constants and its eigenvalues are known as Floquet-multipliers. When all these multipliers are negative, this system is said to be stable. With [7] the Floquet parameters can be found. In order to use that method, the system (16) should be written into one differential equation (Appendix E). The parameters of this equation should meet the condition written in Appendix E. Otherwise, this method can not be applied. However, time was too short to calculate these parameters.

The conclusion of this stability analysis is that (15) gives abound from which the system will be unstable, although it may be lower in reality. However, the Floquet theory could give a more precise condition for stability.

7. Speed of convergence

Another important issue, next to stability, is the speed of convergence of λ. Looking at the system in Figure 7 it can be noticed that there is a pole-zero cancellation between the vehicle and the band-pass filter and leaves a filter with two poles. A *simplified* structure of this system is shown in Figure 11.

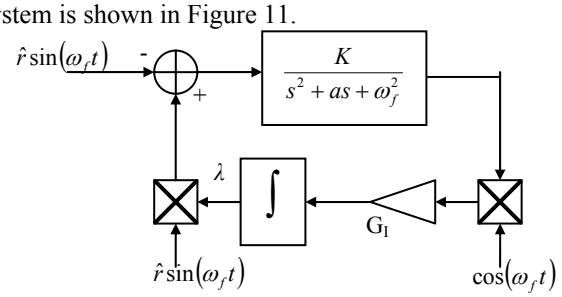

Figure 11: Simplified scheme of the system

The two multiplications and integrator can be called a modulated-integrator. Meaning that it integrates the amplitude of the frequency ω_f and will compensate any input of that frequency. When the system is further reduced by removing the low-pass filter of Figure 11, a simple feedback system with a gain and an integrator is left. The response of λ to $\hat{r}\sin(\omega_f t)$ as input is:

$$\lambda = 1 - e^{-G_I \int (\hat{r}\sin(\omega_f t))^2 dt} \tag{23}$$

This system does not have a limit to its convergence speed, the higher G_I, the faster the input is compensated by the feedback-loop. If the second-order low-pass filter is put back into the system it will influence the speed. Due to the fact that the filter has two poles with real part a, this filter will have a time-constant of $1/a$. The result to the system of Figure 7 is that the *maximum* speed of convergence is limited by the band-pass filter with $1/a$ as time-constant. Which is $1/\omega_f$ if it is a critical damped filter. Thus for the sake of convergence it is best to have a high input frequency ω_f.

Remark: The sensor, that measures the engine speed, is a digital sensor, meaning that it has a certain sample-time T_s. According to Nyquist this sensor can only measure signals until $\omega_s = 4\pi/T_s$ [rad/s]. Thus the sensor puts a very hard limit to the period T_f of dP and also to the maximum speed of convergence.

8. Noise analysis

The noise is modelled by adding it to the engine speed v. The analysis of noise can be divided into three different kinds of noise:

- disturbances near ω_f
- disturbances far from ω_f
- quantisation noise

A. Disturbance near ω_f

If there is a disturbance d of frequency ω_f, df will not only cancel the response of ω_f on P but also of d. To see the influence of d on λ, d is transferred from v to the power summation, shown in Figure 12.

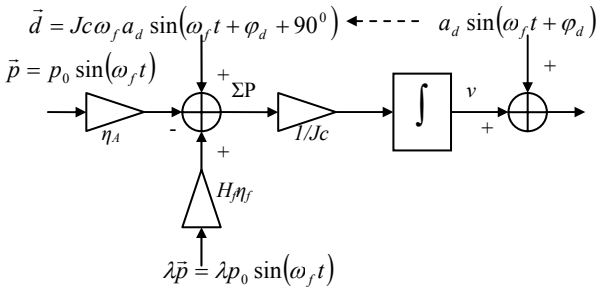

Figure 12: Disturbance on v translated to input

The three inputs can be seen as vectors. Only that part of the vectors that are in the same direction as df will be compensated by df, shown in Figure 13

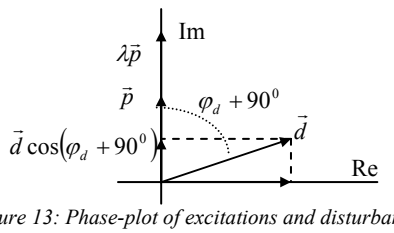

Figure 13: Phase-plot of excitations and disturbance

With the decomposition of d in the direction of p, equilibrium of this system (ΣP=0) results in:

$$H_f\eta_f\lambda p_0 - \eta_A p_0 + a_d Jc\omega_f \cos(\varphi_d + 90^0) = 0$$
$$\Rightarrow \lambda = \frac{\eta_A}{H_f\eta_f} - \frac{a_d Jc\omega_f}{H_f\eta_f p_0}\sin(\varphi_d) \quad (24)$$

Equation (24) shows that indeed a disturbance at the same frequency as the fundamental of dP results in a wrong identification of the IFR. It also shows that when p_0 is very large compared to a_d, the influence of d on λ can be neglected. One thing that can be done about this error is estimating d when $dP = 0$. When $dP = 0$ and v is multiplied with both $2\sin(\omega_f t)$ and $2\cos(\omega_f t)$, an estimation can be made of $d = \hat{d}\sin(\omega_f t + \hat{\varphi}_d)$

$$\left.\begin{aligned} a_d \sin(\omega_f t + \varphi_d)2\sin(\omega_f t) &\approx a_d \cos\varphi_d \\ a_d \sin(\omega_f t + \varphi_d)2\cos(\omega_f t) &\approx a_d \sin\varphi_d \end{aligned}\right\}$$
$$\Rightarrow \begin{cases} \hat{d} = 2\sqrt{(a_d\cos\varphi_d)^2 + (a_d\sin\varphi_d)^2} \\ \hat{\varphi}_d = \arctan\left(\dfrac{a_d\sin\varphi_d}{a_d\cos\varphi_d}\right) \end{cases} \quad (25)$$

The estimated d is subtracted from the measured v. The reason is that the identification-box then receives the response of dP on v without a disturbance and stability of dP is guaranteed. This will only work when d does not changes rapidly.

Remark: Not only a disturbance at ω_f is unfavourable for identification, but also all other odd harmonics of ω_f. Suppose that the disturbance has a frequency of $3\omega_f$, then after the two multiplications the main part of it is fed back into the system as $3\omega_f$ but there is also a part that is fed back as ω_f. To calculate its influence let us first transfer this component from v to the input, the same way as shown in Figure 12. With the help (52b) the influence of a harmonic on the input of the system can be calculated (starting from s_0 and going to s_{-2}). If the disturbance is:

$$d = d_1\sin(\omega_f t + \varphi_1) + d_3\sin(3\omega_f t + \varphi_3) \quad (26)$$

Equation (24) results in:

$$H_f\eta_f\lambda p_0 - \frac{p_0}{\eta_A} + d_1 Jc\omega_f\cos(\varphi_1 + 90^0) + d_3 Jc3\omega_f\left(T_{0,-1}T_{-1,-2}\right)\cos(\varphi_3 + 90^0) = 0 \quad (27)$$

However, it is assumed that the influence of all harmonics, including $3\omega_f$, can be neglected because all filters are low-pass filters.

b. Disturbance far away from ω_f

The influence of noise on λ depends on a number of parameters. The ones of interest are the amplitude of the input signal p_0, the fundamental frequency ω_f and the integrator's gain G_I. The influence of G_I and p_0 is best explained with Figure 7. The multiplication with $p_0\sin(\omega_f t)$ is divided into a multiplication with $\sin(\omega_f t)$ and after that a gain p_0. The noise influence shall be discussed just in front of the gain p_0, which will be called λ' ($=\lambda\sin(\omega_f t)$).

G_I is both in the loop and in the direct path between d and λ'. So if G_I is increased, the noise on λ' is increased as well. The parameter p_0 is also in the loop but not directly between d and λ'. Thus if this is increased it will not do that much to the noise on λ'. However, if p_0 is increased, G_I can be decreased to have the same convergence time. This because the convergence time is dependent on the loop-gain, which will remain the same. So indirectly, increasing p_0 in order to decrease G_I will reduce the noise.

The influence of ω_f on λ' is best shown with the function $Z_\lambda(\omega)$ from d to λ'.

$$Z_\lambda(\omega) = \frac{-G_I H_{BPF}\dfrac{\omega_f}{\omega^2 - \omega_f^2}}{1 - H_{P_0}\left(\left(e^{j\frac{\pi}{2}}Z_{C_{+1}}(\omega)\right) - \left(e^{j\frac{\pi}{2}}Z_{C_{-1}}(\omega)\right)\right)} = \frac{-G_I\dfrac{\omega_f}{\omega^2 - \omega_f^2}a(j\omega)}{(j\omega)^2 + a(j\omega) + \left(\omega_f^2 + G_I\dfrac{aH_f\eta_f p_0}{Jc}\dfrac{\omega_f}{\omega^2 - \omega_f^2}\right)} \quad (28)$$

If '$(j\omega)$ is replaced by s' the function looks similar to a band-pass filter with frequency-dependent gain and poles. It is also seen that G_I is indeed in the direct path (numerator) as well as the loop (denumarator) and that p_0 is only in the loop.

The influence of ω_f on the function $Z_\lambda(\omega)$ is not easy. The high-frequency region will not change that much if ω_f is changed, but the low region has a gain linear to $1/\omega_f$. Thus increasing ω_f has a positive effect on low-frequency noise. However, to get the same convergence speed, G_I has to be increased if ω_f is increased. Therefore little changes are expected in the low frequency region when ω_f is changed. The most interesting region for the noise is that around ω_f. This is illustrated with an example.

Example 1

Let's take an example in which the function $Z(\omega)$ is in its instability point, thus G_I is such that the equality in (15) holds.

$$Z_\lambda(\omega) = \frac{Jc}{H_f\eta_f p_0}\frac{-\dfrac{\omega_f^4}{\omega^2 - \omega_f^2}(j\omega)}{(j\omega)^2 + a(j\omega) + \left(\omega_f^2 + \dfrac{\omega_f^4}{\omega^2 - \omega_f^2}\right)} \quad (29)$$

For high frequencies this $Z_\lambda(\omega)$ is $\sim 1/\omega^3$ (=-60dB/dec). For low frequencies this function will go to some constant that is linear to ω_f^2. Low-frequency noise is the one we should be concerned about in this special case. Notice that when G_I is less then the stability point, $Z_\lambda(\omega)$ is linear to ω for low frequencies (=-20dB/dec).

Two simulations of this filter were done. The first one shows the magnitude-plot for G_I such that equality in (15) holds, in the second one G_I was less. Other parameters were chosen similar to reality and $\omega_f = 1$ Hz.

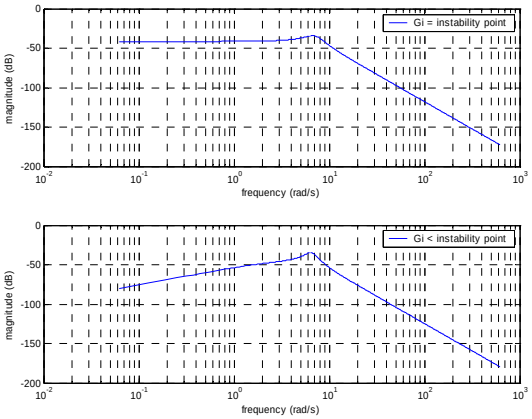

Figure 14: Noise transfer to λ dependent on G_I.

Figure 14 shows that the high frequency domain does not change much in behaviour when G_I is not at its instability point (both decay with $\sim 1/\omega^3$). Nevertheless, for low frequencies, the behaviour does change.

Example 2

In this example the influence of ω_f is looked at. For that two simulations were done. In the first simulation $\omega_f = 1$ Hz and in the second simulation ω_f = 10 Hz. To compensate the decrease in speed of convergence, G_I was ten times bigger in the second simulation. Figure 20 shows their transfer function.

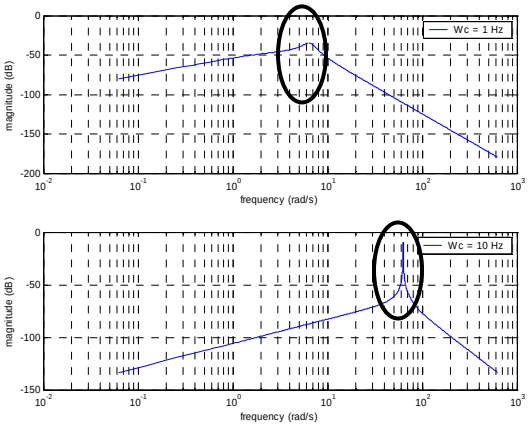

Figure 15: Transfer function for two different ω_f.

The plot in Figure 15 shows that more noise can be expected from frequencies near ω_f when ω_f is increased (the second plot has a higher peak). This is caused by the increased G_I to keep the same speed of convergence when ω_f is increased.

c. Quantisation noise

The sensor that measures the speed introduces quantisation levels. Let's call the difference between these levels the quantisation step q. The influence of dP on the engine speed therefore has to be bigger then q, otherwise it may not be measured. Moreover, the vehicle is assumed to be an integrator, which means that the higher the frequency, the less response on the speed. So the resolution of the sensor q puts a limit to ω_f.

If p_0 is the amplitude of the fundamental of dP, its response on v should have at least an amplitude of $q/2$ to see a change in the measured engine speed.

$$\frac{\eta_A p_0}{Jc\omega_f} \geq \frac{q}{2} \Rightarrow p_0 \geq q\frac{Jc\pi}{\eta_A T_f} \tag{30}$$

Assume that the duty cycle is 15% at minimum (if P_{max} = 1500 W => $P_0 \approx 200$ W). The minimum amplitude of p_0 to detect a change on v can be calculated with (3).

$$p_0 \approx 0.27 P_{\max} \left\{ = \sqrt{a_1^2 + b_1^2}\, P_{\max} \middle| D = 0.15 \right\} \tag{31}$$

Substituting (30) in (31) results in a minimal period T_f:

$$T_f \geq q\frac{Jc\pi}{0.27\eta_A P_{\max}} \tag{32}$$

But there is more influence of the quantisation noise, because eventually it will measure the response of df and dP together. The system controls the response on v to 0, only 0 can not be measured. Due to the quantisation steps, the system can control the response to a minimum of $\pm q/2$ instead of 0. This means that there will be an error on λ which is relative to p_0 and q. If the sensor was perfect and could measure 0, in equilibrium would hold:

$$\frac{1}{Jc\omega_f}\left(H_f \eta_f \lambda p_0 - \eta_A p_0\right) = 0 \tag{33}$$

But due to the quantisation steps:

$$\frac{1}{Jc\omega_f}\left(H_f \eta_f \lambda p_0 - \eta_A p_0\right) = \pm\frac{q}{2} \tag{34}$$

Therefore λ will converge to:

$$\lambda = \frac{\eta_A}{H_f \eta_f} \pm \frac{qJc\omega_f}{2H_f \eta_f p_0} \tag{35}$$

Equation (35) shows that when q = 0, λ will converge to its original value. To have little error on λ, p_0 should be as high as possible and ω_f as low as possible. This could be expected.

Remark: Suppose that not the angular speed v but the angle θ itself is measured in quantisation steps $\Delta\theta$. Then the maximum error e in speed is not the constant q anymore, but related to the sampling time of the sensor. Most likely the vehicle will measure the time (in n steps T_s) between two phase-steps. In the worst case the real time between two phase-steps was just below $(n+1)T_s$, and the sensor would measure nT_s. Thus the error in speed is:

$$e = v - \hat{v} \leq \frac{\Delta\theta}{(n+1)T_s} - \frac{\Delta\theta}{nT_s} = \Delta\theta\left(\frac{1}{n(n+1)T_s}\right)$$

9. Simulation

In addition to the analyses in previous sections, simulations of the system are done. First the parameters are inserted into the model. Second simulations are done without noise which concerns instability, the speed of convergence and the correct IFR. At third, noise will be added to the system to validate the noise analysis in Section 8.

a. Substitution of the parameters

Parameters of the vehicle are given in Table 1:

$m_{vehicle}$	1500 [kg]
gear-ratio	{3.4 2.1 1.5 1.0 0.8 0.6}
final-drive ratio	4
wheel radius	0.3 [m]
wheel + axle inertia	3.3 [kgm^2]
gearbox and final-drive inertia	0 [kgm^2]

Table 1:Vehicle parameters

Under the condition that the vehicle is driving its fifth gear, the equivalent inertia of the vehicle J = 24 kgm^2. When the vehicle is driving 30 m/s, the engine speed v equals 300 rad/s.

In reality the efficiencies η_f and η_A are not constant but there is a fuel-map for η_f and an inverse alternator-map for η_A. Both efficiencies are modelled as elliptical contours dependent on the engine speed and their input power. The fuel-map is modelled with the following function:

$$r_f(v,P_f) = D_{v,f}(v - v_{f0})^2 + D_{T,f}\left(\frac{P_f}{v} - T_{f0}\right)^2$$

$$\eta_f(v,P_f) = \eta_f(opt) - \frac{r_f(v,P_f)}{r_f(0)} \qquad (36)$$

and the inverse alternator-map with:

$$r_A(v.P) = D_{v,A}(v - v_{A0})^2 + D_{P,A}(P - P_{A0})^2$$

$$\eta_A(v,P) = \eta_A(opt) + \frac{r_A(v,P)}{r_A(0)} \qquad (37)$$

The value of these parameters are selected as:

$\eta_f(opt)$	0.3	$\eta_A(opt)$	1.25
$D_{v,f}$	1/125^2 [s^2/rad^2]	$D_{v,A}$	1/210^2 [s^2/rad^2]
$D_{T,f}$	1/100^2 [1/N^2]	$D_{P,A}$	1/400^2 [1/W^2]
v_{f0}	262 [rad/s]	v_{A0}	230 [rad/s]
T_{f0}	100 [N]	P_{A0}	600 [W]
$r_f(0)$	20	$r_A(0)$	10

Table 2: Efficiency parameters

H_f is set to 42500 J/g. Due to the fact that both efficiencies are a function of their input, the amplitude of the input will effect the steady state value of λ. This is because λ is related to the average of both efficiencies during the calculation of λ. If the efficiencies were constants, λ would always go to the same value at a certain operation point of the vehicle (independent of dP). But due to the fact that they change along with dP, this is not the case anymore, although the value of λ still gives the IFR.

The band-pass filter is critical damped and depends on ω_f (= $2\pi/T_f$).

$$H_{BPF} = \frac{2\omega_f s}{s^2 + 2\omega_f s + \omega_f^2} \qquad (38)$$

The compromise between a 2nd-order filter and a higher one (for better noise-reduction) is based on the speed of removing c and the total phase-shift of the filter. A big phase-shift introduces a bigger chance to encircle -1 in the Nyquist-plot. A 2nd-order filter is the fastest in removing c and has the less phase-shift.

The nominal electrical power P_0, provided by the alternator, is 400 W. Together with the calculated friction, the nominal fuel-injection f_0 can be determined.

b. Simulations without noise

Both efficiencies are a function of their inputs and not constant gains, thus λ will be different compared to (9). Suppose both efficiency functions are written as first order Taylor expansions around the operating point (c,P_0) and (c,P_{f0}). Thus with constant speed $v = c$.

$$\eta_A(dP) \approx \eta_A(c,P_0) + \left.\frac{\delta\eta_A}{\delta P}\right|_{(c,P_0)} dP$$

$$\eta_f(dP_f) \approx \eta_f(c,P_{f0}) + \left.\frac{\delta\eta_f}{\delta P_f}\right|_{(c,P_{f0})} dP_f \qquad (39)$$

The power equation of the car (P_A+P_f+$P_{friction}$) becomes:

$$(P_0 + dP)\left(\eta_A + \frac{\delta\eta_A}{\delta P}dP\right) - (f_0 + df)H_f\left(\eta_f + \frac{\delta\eta_f}{\delta P_f}dP_f\right) + P_{friction} \qquad (40)$$

Assuming that the nominal powers cancel each other and that dP^2 and $dfdP$ can be neglected, the equilibrium of (40) together with ($df = \lambda dP$) results in:

$$\underbrace{\left(P_0\frac{\delta\eta_A}{\delta P}dP + \eta_A dP\right)}_{dP_A} - H_f\left(f_0\frac{\delta\eta_f}{\delta P_f}dP_f + \eta_f\lambda dP\right) = 0 \qquad (41)$$

The excitation on the fuel power dP_f has to cancel the excitation of the alternator power dP_A at ω_f, therefore $dP_f = dP_A = \left(P_0\frac{\delta\eta_A}{\delta P}dP + \eta_A dP\right)$. The solution of (41) gives:

$$\lambda \approx \frac{\eta_A}{H_f\eta_f} + \frac{P_0}{H_f\eta_f}\frac{\delta\eta_A}{\delta P} - \frac{f_0\left(P_0\frac{\delta\eta_A}{\delta P} + \eta_A\right)}{H_f\eta_f}\frac{\delta\eta_f}{\delta P_f} \qquad (42)$$

In the first simulation dP is a sine (thus no harmonics) with an amplitude p_0 = 100 W and T_f = 1s. In this situation the engine's operation point η_f is equal to 0.28. The stability bound of G_I according to (15) is 0.23 and from (42) λ = 9e-5 [g/J].

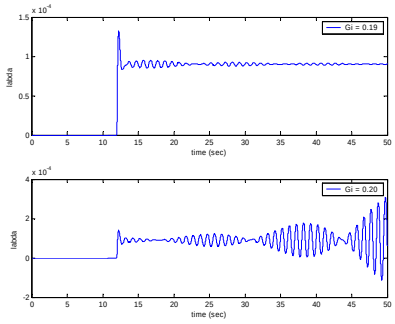

Figure 16: Response of λ for different G_I

Simulations in Figure 16 show that the instability point is at G_I = 0.19 (for that G_I the response of λ still converges, because G_I = 0.20 it diverges). Therefore it can be said that (15) is a good approximation for instability. Figure 16 shows also that (42) is a good representation for λ.

Analysis in Section 7 showed that the maximum speed of convergence is linear to the input frequency. An input frequency of 1 Hz is compared to 10 Hz in Figure 17. In order to make the two simulations comparable to each other G_I is equal to 0.05 for 1 Hz and $0.05*10^2$ ($\sim\omega^2$) for 10 Hz (one ω to compensate the extra decay in the vehicle and one ω to increase the speed of convergence). G_I is in both cases the instability point divided by 4.

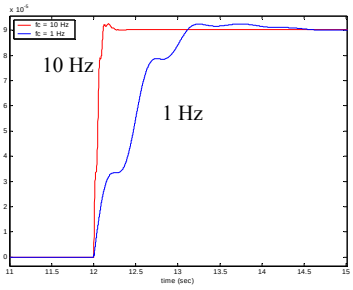

Figure 17: Response of λ for different frequencies

The response for ω_f = 10 Hz is indeed about 10 times faster than for ω_f = 1 Hz. According to the analysis this is caused by the band-pass filter rather then the first harmonic of *dP*. To verify this observation, T_f was set to 1 second. In the first simulation the band-pass filter had a centre-frequency of 1 Hz and G_I = 0.05. In the second one the centre-frequency of the band-pass filter is at 10 Hz and G_I is increased to 0.5 to compensate the extra decrease in the band-pass filter. Figure 18 shows the results of these simulations.

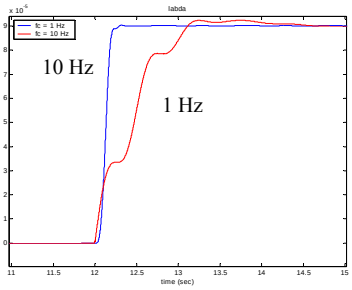

Figure 18: Response of λ for different band-pass filters

In the fastest response of λ in Figure 18 the band-pass filter had a centre-frequency of 10 Hz instead of 1 Hz. Thus the band-pass filter puts the limit on the speed of convergence, as shown in Section 7.

The sine-wave of *dP* is replaced with a PWM to see the influence of harmonics at the input. T_f was set to 1 second. Correlation is done with a sine-wave of ω_f and λ is multiplied with the fundamental of *dP*. The amplitude of the fundamental p_o is changed and according to (42) λ converges again to 9e-5 [g/J]. Figure 19 shows that the harmonics of the PWM do not affect the steady state value of λ, because it is the same as in Figure 17 and 18. However, if only the fundamental is compensated by *df* the higher harmonics remain on the input of the vehicle. It is not likely that these harmonics together will have a zero mean. Thus the vehicle is affected in its drivability if *dP* is a PWM, if *dP* is a sine the drivability is not affected.

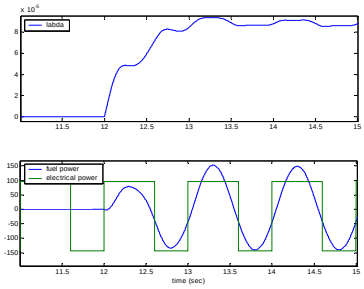

Figure 19: Response of λ and df for a PWM signal of dP

c. Simulations with noise

According to the analysis in Section 8 quantisation noise causes an error on the identification of λ. To the simulation-model a quantizer is added to the engine speed *v*. Simulations were done with two different levels for *q* (0.04 and 0.004), T_f = 1 s, *dP* was increased to an amplitude of 700 W and G_I = 0.007. The nominal power P_0 = 900 W and λ should converge to 1.25e-4 [g/J].

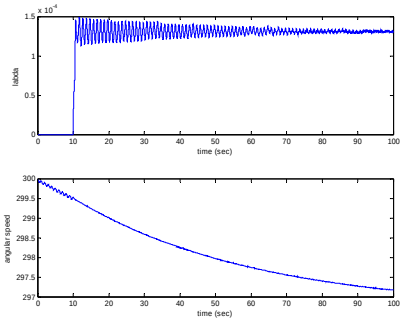

Figure 20: Response of λ and v for q = 0.004

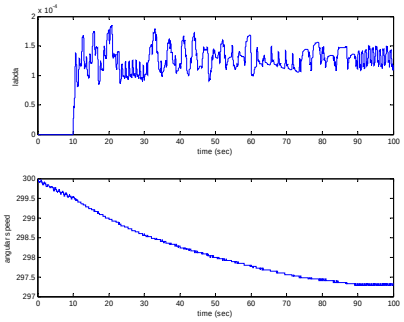

Figure 21: Response of λ and v for q = 0.04

The plots of λ in Figure 20 and 21 show the effect of the quantizer. Especially when *q* is large (Figure 21) the noise on λ is significant. But beside that, λ goes to a higher value then (42) indicates, 1.3e-5 [g/J] instead of 1.25e-5 [g/J]. The main reason is that a first order Taylor expansion of the efficiency functions (39) is not exact enough when it is far from its point of operation. Which is the case when *dP* is 700 W.

Finally the speed of convergence was simulated as a function of noise energy. The noise its Power Spectral Density was in all cases the same (10e-6 W until 1000 Hz) and the momentary error on λ was limited to $5*10^{-10}$

[(g/J)^2]. The gain G_I was adjusted to meet that limit on λ and an estimation was done on the speed of convergence for different T_f.

T_f (sec)	speed (sec)
2	10
1.6	1.5
1	1
0.4	3
0.2	6

Table 3: Convergence speed

Table 3 shows that there is an optimum in T_f to have the fastest convergence. The higher the frequency, the faster convergence, but also the more noise in the area of interest. Thus if a fast calculation of λ is wanted, there will be a trade-off between a high frequency and noise-influence. To give a feeling of the amount of noise on λ, a plot of its response with $T_f = 1$ s is shown in Figure 22.

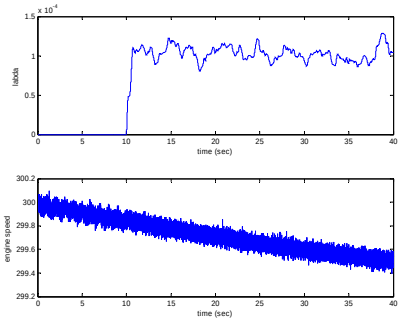

Figure 22: Response of λ and v with noise

10. Conclusions

The system designed in this paper will calculate the IFR λ online. The advantage of this design is that with a small signal on the input, identification of a specific parameter is done reasonable fast. The largest contribution to that is the correlation technique. Also stability can be predicted according to (15). Although this value is not exact, it is a good approximation. Another advantage of this system is the ability to handle a PWM input, which provides more information than a sine-input.

The accuracy of λ is related the one quantisation step q of the sensor. In a perfect situation ($q = 0$) the system will control the response on v to 0, resulting in an errorless λ. In all other situations the system will control the output v between $\pm q/2$, undetectable for the sensor and resulting in an error on λ (35). A disturbance at ω_f, or an harmonic of that, can also lead to an error on λ. Its effect can be compensated by first measuring this disturbance and then subtract it from v.

It is shown that inputs with a higher frequency result in a faster convergence. However, for a vehicle there are a number of drawbacks that limit the speed of convergence of λ. The sensor is limited in bandwidth and resolution. Bandwidth gives a hard limit to which frequencies can be measured. Resolution because the higher the input frequency, the smaller the response on the engine speed. Another reason that limits the speed of convergence is noise. If the ω_f increases, G_I also has to be increased to have a faster convergence. This will result in more noise-power on λ.

Future work can be to analyse the stability of the system using the Floquet-method of [7] or an improved method to calculate the Floquet-multipliers. The correlation can be improved by measuring the phase φ of the response of dP on v. If the multiplication is then done with $\sin(\omega_f t+\varphi)$, the normalized expectation is always near 1. A final recommendation is related to the three 'inputs' of the system (dP and the 2 multiplications). An analysis of which signal, sine or PWM, on which input can help in improving the performance of the identification.

References

[1] Stalnaker D.
Hybrid Electric Vehicle Analysis.
NASA Lewis Research Center, Cleveland, Online User's Guide.
http://downloads.openchannelfoundation.org/projects/HEVA

[2] Fourier Series: square wave.
http://mathworld.wolfram.com/FourierSeriesSquareWave.html

[3] Damen A.A.H.
Syllabus 'Modern Control Theory'.
TU Eindhoven, Department or Electrical Engineering.

[4] Sanders J.A. and F.A. Verhulst
'Averaging methods in nonlinear dynamical systems'.
New York: Springer, 1985.

[5] Guckenheimer J. and P. Holmes.
'Nonlinear oscillations, dynamical systems and bifurecations in vector fields'.
New York: Springer, 1983.

[6] Verhulst F.A.
'Nonlinear Differential Equations and Dynamical Systems'.
Berlin: Springer, 1996.

[7] Kloet P.A. van der
Thesis: Modal solutions for Linear Time Varying systems. (page 43-46)
TU Delft, department of electrical Engineering 2002

Appendix A

A.1. Analysis of a sinusoidal-multiplication

Before the system in Figure 1 is analysed it is put in a more general framework, that way the analysis is not restrained to one system. This general system, shown in Figure 23, is a feedback system consisting of a filter and multiplication with $a\sin(\omega_f t)$.

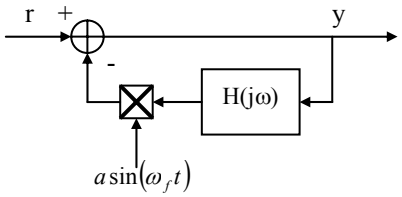

Figure 23: Feedback system with wave multiplication

The aim is to find a model of this system. Two analyses are done. The first one is to give the reader insight in the model. The second one is more mathematical which will show that the same model can be derived starting from another point of view. First notice that y is linear to r because when $H(j\omega) = 1$, the response of y is:

$$y = \frac{1}{1 + a\sin(\omega_f t)} r \tag{43}$$

Thus when the frequency response of this system is known, the response for all signals is known.

a. Analysis 1

In the first analysis each multiplication with a sine is seen as a frequency-shifter. Suppose $r = \sin(\omega_0 t + \varphi)$, after one loop r returns in the output y as:

$$\begin{aligned} &\sin(\omega_0 t + \varphi) \underset{1-loop}{\rightarrow} -a\sin(\omega_f t)|H(j\omega_0)|\sin(\omega_0 t + \varphi + \varphi_{H(\omega_0)}) \\ &= \frac{a}{2}|H(j\omega_0)|\cos((\omega_0 + \omega_f)t + \varphi + \varphi_{H(\omega_0)}) \\ &-\frac{a}{2}|H(j\omega_0)|\cos((\omega_0 - \omega_f)t + \varphi + \varphi_{H(\omega_0)}) \end{aligned} \tag{44}$$

Equation (44) shows that in one loop r goes through $H(j\omega)$, is shifted in frequency, is added with a phase of -90^0 (=1/j) and is multiplied with $\pm a/2$. Suppose the signal s_n and parameter h_0 are complex and defined as:

$$h_0 = \frac{a}{2}H(j\omega_0); \quad s_n = e^{j((\omega_0 + n\omega_f)t + \varphi)} \tag{45}$$

(45) substituting in (44) results in (Appendix B):

$$s_0 \underset{1-loop}{\rightarrow} \frac{1}{j}h_0 s_{-1} - \frac{1}{j}h_0 s_{+1} \tag{46}$$

Equation (46) is valid for all frequencies ω_0, thus ω_0 can also be replaced by $\omega_0 + n\omega_f$. When h_n is defined as:

$$h_n = \frac{a}{2}H(j(\omega_0 + n\omega_f)) \tag{47}$$

A more general form of the system in Figure 23 is:

$$s_n \underset{1-loop}{\rightarrow} \frac{1}{j}h_n s_{n-1} - \frac{1}{j}h_n s_{n+1} \tag{48}$$

Equation (48) shows the next output of the system given the present output. This means that a tree-structure of the output y can be made, of this system in equilibrium, starting from s_0.

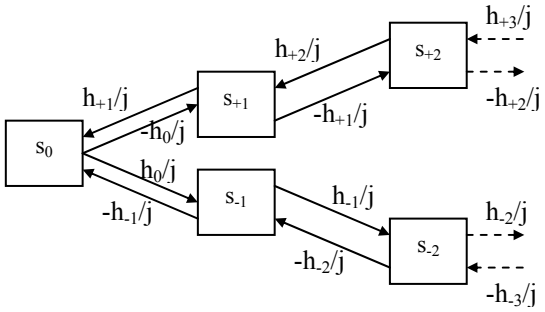

Figure 24: Tree of harmonics at the output

In equilibrium each signal s_n has a certain amplitude c_n. Figure 24 provides the relation between the amplitudes c_n of y by adding the arrows that point towards some s_n:

$$c_n = -\frac{1}{j}h_{n-1}c_{n-1} + \frac{1}{j}h_{n+1}c_{n+1} \tag{49}$$

From (49) a model of the system can be derived. This model consists of two parts, a function $Z(\omega)$ and an input. The function will act the same for any harmonic s_n. However, the harmonics that are generated in the general system are not generated in $Z(\omega)$. To correct that, these harmonics are added to the input of the function. What their amplitude and phase must be is considered after $Z(\omega)$ of the model is derived.

Let's start with an easy model and cut-off the tree for all n bigger than ±1. In that case the model covers only the response of s_{-1}, s_0 and s_{+1}. The function of the model is calculated by assuming that r_o is the input's amplitude at s_0. From (49) follows:

$$\left.\begin{aligned} c_0 &= -\frac{1}{j}h_{-1}c_{-1} + \frac{1}{j}h_{+1}c_{+1} + r_0 \\ c_{-1} &= \frac{1}{j}h_0 c_0 \\ c_{+1} &= -\frac{1}{j}h_0 c_0 \end{aligned}\right\}$$

$$\begin{aligned} &\Rightarrow c_0 = h_0(h_{-1} + h_{+1})c_0 + r_0 \\ &\Rightarrow Z(\omega) = \frac{c_0}{r_0} = \frac{1}{1 - h_0(h_{-1} + h_{+1})} \end{aligned} \tag{50}$$

The harmonics still have to be added to the input of $Z(\omega)$. For that, the value of each harmonic **not** generated after itself is calculated. Because once it is generated its contribution to y will follow from $Z(\omega)$ as shown in (50). For clarity each harmonic of the input of $Z(\omega)$ is called r_n. The tree of Figure 24 shows how to calculate the signals r_{-1} and r_{+1}. The relation between r_{-1} and r_0 is the transfer from s_0 to s_{-1},, with $r_0 = r$ (input of the system)

$$r_{-1} = \frac{1}{j}h_0 \frac{1}{1 + h_0 h_{+1}} r_0 \quad r_{+1} = -\frac{1}{j}h_0 \frac{1}{1 + h_0 h_{-1}} r_0 \tag{51}$$

From (50) and (51) the model can be made.

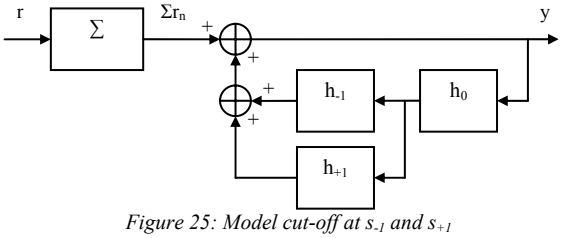

Figure 25: Model cut-off at s_{-1} and s_{+1}

From Figure 25 and (50) the model covering all harmonics can be extracted. The function of the model is shown in Figure 26, which is a translation of the function in (52a) into a graphical form.

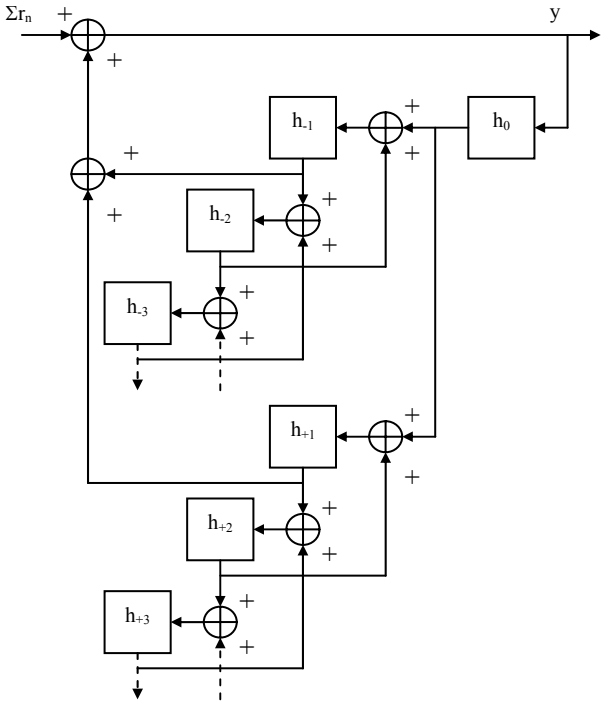

Figure 26: Transfer of the model

The function of this transfer from Σr_n to y is:

$$Z(\omega)=\frac{1}{1-h_0(h_-+h_+)} \tag{52a}$$

with

$$h_-=\frac{h_{-1}}{1-h_{-1}\left(\frac{h_{-2}}{1-h_{-2}(...)}\right)}$$

$$h_+=\frac{h_{+1}}{1-h_{+1}\left(\frac{h_{+2}}{1-h_{+2}(...)}\right)}$$

The harmonics Σr_n have to be calculated, which is equivalent to the calculation of r_{-1} and r_{+1}. As an example r_{-3} is calculated. This means that the start is at s_0 and goes to s_{-3}, shown in Figure 27.

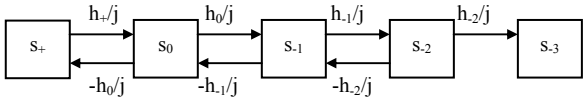

Figure 27: Going from s_0 to s_{-3}

If $T_{n,n-1}$ is the transfer of the system from s_n to s_{n-1}, then $r_n = T_{n,n-1}r_{n-1}$. The value of r_{-3} starting from r_0, is (52b) product of all transfers T between r_0 and r_{-3}: $T_{-3,-2}T_{-2,-1}\,T_{0,-1}$.

$$T_{0,-1}=\frac{1}{j}\frac{h_0}{1-h_+h_0}$$

$$T_{-2,-1}=\frac{1}{j}\frac{h_{-1}}{1-h_{-1}\left(\frac{h_0}{1-h_+h_0}\right)}$$

$$T_{-3,-2}=\frac{1}{j}\frac{h_{-2}}{1-h_{-2}\left(\frac{h_{-1}}{1-h_{-1}\left(\frac{h_0}{1-h_+h_0}\right)}\right)}$$

b. Analysis 2

The second analysis is a more mathematical one. If the input r of the system in Figure 7 is given by:

$$r=\hat{r}\sin(\omega_0 t) \tag{53}$$

The output y consists of the frequencies $\omega_0+n\omega_f$:

$$y=\sum_{k=-\infty}^{\infty}a_k\sin\left((\omega_0+k\omega_f)t+\varphi_k\right)=\mathrm{Im}\left\{\sum_{k=-\infty}^{\infty}c_k e^{j(\omega_0+k\omega_f)t}\right\} \tag{54}$$

In equilibrium of the system holds:

$$y=r-a\sin(\omega_f t)\cdot H(j\omega_y)\cdot y \tag{55}$$

If r is put to zero, substituting (53) and (52) in (53) gives (see Appendix C):

$$\sum_{k=-\infty}^{\infty}c_k e^{j(\omega_0+k\omega_f)t}=$$

$$-\frac{a}{2j}\sum_{k=-\infty}^{\infty}\left\{c_k H\left(j(\omega_0+k\omega_f)\right)\left(e^{j(\omega_0+(k+1)\omega_f)t}-e^{j(\omega_0+(k-1)\omega_f)t}\right)\right\}$$

Combining equal frequencies results in an equation for each c_k. Taking the definition of h_n from (47), gives:

$$c_k=\frac{-1}{j}\left(h_{k-1}c_{k-1}-h_{k+1}c_{k+1}\right) \tag{56}$$

This result is equal to (49).

c. Simulations model versus general system

The model in Figure 26 is simulated versus the general system in Figure 23. The squared error between the output y of both systems is plotted in Figure 28. On the x-axis is the number of the harmonics, so if $x = 0$, only s_0 was used, if $x = 2$, the model system went from s_{-2} until s_{+2}. The used parameters are: $\omega_0 = 3$ Hz, $\omega_f = 10$ Hz and $a = 0.8$. The filter of the system is: $H(j\omega)=\frac{50}{j\omega+100}$.

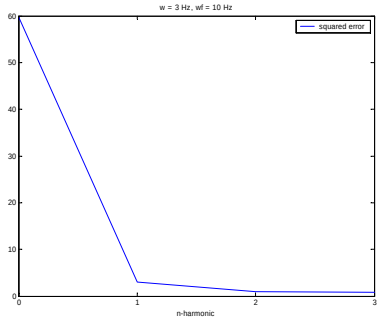

Figure 28: Error between model and system

From Figure 28 can be concluded that the model of Figure 26 is a good description of the general system in Figure 23. The original system of Figure 1 can now be transformed into this model.

A.2. System model

As said earlier, the fundamental that goes into the vehicle will get a phase-shift of -90^0 and the correlation-block chooses $\cos(\omega_f t)$ as multiplicand. The system of Figure 7 is shown again for clarity.

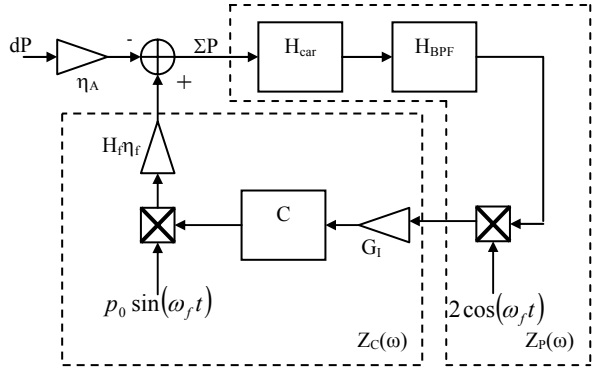

Figure 29: Identification system

The fundamental of dP is $p_0\sin(\omega_f t)$. This system has to be converted into the model of the general system in Section A.1. This is established by taking the loop of the general system in Figure 23 'twice at a time' instead of once, both with different filters. These filters are:

$$Z_{P_n}(\omega) = H_{BPF}\left(j(\omega + n\omega_f)\right)H_{car}\left(j(\omega + n\omega_f)\right) \qquad (57a)$$

$$Z_{C_n}(\omega) = G_I \frac{p_0\eta_f H_f}{2} C\left(j(\omega + n\omega_f)\right) \qquad (57b)$$

The general system of Figure 23 is fed back with a minus sign. To that end a minus sign is put in front of each sinusoidal multiplication of the system in Figure 29. If further the first multiplication is taken as $-2\sin(\omega_f t)$ instead of $-2\cos(\omega_f t)$, the system is put into the general form of Figure 23. The difference between multiplying with $\sin(\omega_f t)$ instead of $\cos(\omega_f t)$ will be taken care of later. The function $Z(\omega)$ of this system analogue to (52a) is:

$$Z(\omega) = \frac{1}{1 - Z_{P_0}(\omega)\left(Z_-(\omega) + Z_+(\omega)\right)} \qquad (58)$$

with

$$Z_-(\omega) = \frac{Z_{C_{-1}}(\omega)}{1 - Z_{C_{-1}}(\omega)\left(\dfrac{Z_{P_{-2}}(\omega)}{1 - Z_{P_{-2}}(\omega)(...)}\right)}$$

$$Z_+(\omega) = \frac{Z_{C_{+1}}(\omega)}{1 - Z_{C_{+1}}(\omega)\left(\dfrac{Z_{P_{+2}}(\omega)}{1 - Z_{P_{+2}}(\omega)(...)}\right)}$$

When the differences between multiplying with $\sin(\omega_f t)$ and $\cos(\omega_f t)$ are known, the function of (58) can be converted to the one of the system in Figure 29.

$$\sin p \sin q = \frac{1}{2}\left(\cos(p-q) - \cos(p+q)\right) \qquad (59a)$$

$$\sin p \cos q = \frac{1}{2}\left(\sin(p-q) + \sin(p+q)\right) \qquad (59b)$$

Comparing the two leads to that when multiplying with $\cos q$, its phase difference with $\sin q$ ($90^0 = e^{j\pi/2}$) is added to $(p+q)$ and subtracted from $(p-q)$. To model this behaviour, the same changes are substituted at $Z_C(\omega)$:

$$Z(\omega) = \frac{1}{1 - Z_{P_0}\left(Z_-(\omega) + Z_+(\omega)\right)} \qquad (60)$$

with

$$Z_-(\omega) = \frac{\left(e^{-j\frac{\pi}{2}} Z_{C_{-1}}(\omega)\right)}{1 - \left(e^{-j\frac{\pi}{2}} Z_{C_{-1}}(\omega)\right)\left(\dfrac{Z_{P_{-2}}(\omega)}{1 - Z_{P_{-2}}(\omega)(...)}\right)}$$

$$Z_+(\omega) = \frac{\left(e^{j\frac{\pi}{2}} Z_{C_{+1}}(\omega)\right)}{1 - \left(e^{j\frac{\pi}{2}} Z_{C_{+1}}(\omega)\right)\left(\dfrac{Z_{P_{+2}}(\omega)}{1 - Z_{P_{+2}}(\omega)(...)}\right)}$$

(60) shows the function of the system in Figure 29. Equivalent to the comparison of (52a) and (60), the calculation of the harmonics of this system can be done by starting from (52b).

Appendix B

The starting equation is:

$$\sin(\omega_0 t + \varphi) \underset{1-loop}{\rightarrow} \frac{a}{2}|H(j\omega_0)|\left\{\cos\left((\omega_0 + \omega_f)t + \varphi + \varphi_{H(\omega_0)}\right) - \cos\left((\omega_0 - \omega_f)t + \varphi + \varphi_{H(\omega_0)}\right)\right\} \qquad (61)$$

With:

$$\sin(\omega_0 t + \varphi) = \mathrm{Im}\left(e^{j(\omega_0 t + \varphi)}\right)$$

$$\cos\left((\omega_0 + \omega_f)t + \varphi + \varphi_{H(\omega_0)}\right) = \mathrm{Im}\left(je^{j\varphi_{H(\omega_0)}} e^{j\left((\omega_0 + \omega_f)t + \varphi\right)}\right) = \mathrm{Im}\left(-\frac{1}{j} e^{j\varphi_{H(\omega_0)}} e^{j\left((\omega_0 + \omega_f)t + \varphi\right)}\right)$$

Equation (61) becomes:

$$e^{j(\omega_0 t+\varphi)} \underset{1-loop}{\rightarrow} \frac{a}{2}\left|H(j\omega_0)\right|\left(-\frac{1}{j}e^{j\varphi_{H(\omega_0)}}e^{j((\omega_0+\omega_f)t+\varphi)}+\frac{1}{j}e^{j\varphi_{H(\omega_0)}}e^{j((\omega_0-\omega_f)t+\varphi)}\right)$$

$$=\frac{a}{2j}\left|H(j\omega_0)\right|e^{j\varphi_{H(\omega_0)}}\left(-e^{j((\omega_0+\omega_f)t+\varphi)}+e^{j((\omega_0-\omega_f)t+\varphi)}\right)$$

$$=\frac{a}{2j}H(j\omega_0)\left(e^{j((\omega_0-\omega_f)t+\varphi)}-e^{j((\omega_0+\omega_f)t+\varphi)}\right) \qquad (62)$$

Substituting

$$h_0=\frac{a}{2}H(j\omega_0);\quad s_n=e^{j((\omega_0+n\omega_f)t+\varphi)}$$

Equation (62) finally becomes:

$$s_0 \underset{1-loop}{\rightarrow} \frac{1}{j}h_0 s_{-1}-\frac{1}{j}h_0 s_{+1} \qquad (63)$$

Appendix C

The output y consists of the frequencies $\omega_0+n\omega_f$:

$$y=\sum_{k=-\infty}^{\infty}a_k\sin\left((\omega_0+k\omega_f)t+\varphi_k\right)=\mathrm{Im}\left\{\sum_{k=-\infty}^{\infty}c_k e^{j(\omega_0+k\omega_f)t}\right\} \qquad (64)$$

In equilibrium of the system holds:

$$y=r-a\sin(\omega_f t)\cdot H(j\omega_y)\cdot y \qquad (65)$$

Multiplying complex values with each other has the following arithmetic rules:
*Re*Re = Re, Im*Im = Re and Re*Im = Im.*

Applying this to (65):

$$\mathrm{Im}\{y\}=\mathrm{Im}\{-a\sin(\omega_f t)\cdot H(j\omega_y)\cdot y\}$$

$$\Rightarrow \mathrm{Im}\{y\}=-\mathrm{Re}\{a\sin(\omega_f t)\}\cdot\mathrm{Im}\{H(j\omega_y)\cdot y\}$$

$$\Rightarrow \mathrm{Im}\{y\}=-\frac{a}{2j}\left(e^{j\omega_f t}-e^{-j\omega_f t}\right)\cdot\mathrm{Im}\{H(j\omega_y)\cdot y\}$$

$$\Rightarrow \sum_{k=-\infty}^{\infty}c_k e^{j(\omega_0+k\omega_f)t}=-\frac{a}{2j}\left(e^{j\omega_f t}-e^{-j\omega_f t}\right)\cdot\sum_{k=-\infty}^{\infty}\left\{H(j\omega_0+k\omega_f)c_k e^{j(\omega_0+k\omega_f)t}\right\}$$

$$\Rightarrow \sum_{k=-\infty}^{\infty}c_k e^{j(\omega_0+k\omega_f)t}=-\frac{a}{2j}\sum_{k=-\infty}^{\infty}\left\{c_k H(j\omega_0+k\omega_f)\left(e^{j(\omega_0+(k+1)\omega_f)t}-e^{j(\omega_0+(k-1)\omega_f)t}\right)\right\} \qquad (66)$$

Appendix D

Suppose $r=\hat{r}\sin(\omega_f t+\varphi)$.

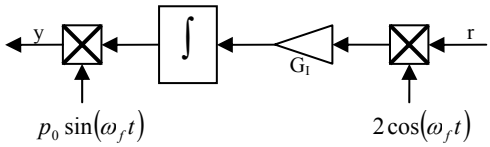

$$y=2p_0G_I\sin(\omega_f t)\int\left(r\cdot\cos(\omega_f t)\right)dt$$

$$=2p_0G_I\sin(\omega_f t)\int\left(\hat{r}\sin(\omega_0 t+\phi)\cdot\cos(\omega_f t)\right)dt$$

$$=\hat{r}p_0{}^2G_I\sin(\omega_f t)\int\left(\sin((\omega_0-\omega_f)t+\phi)+\sin((\omega_0+\omega_f)t+\phi)\right)dt$$

$$=-\hat{r}p_0{}^2G_I\sin(\omega_f t)\left(\frac{1}{(\omega_0-\omega_f)}\cos((\omega_0-\omega_f)t+\phi)+\frac{1}{(\omega_0+\omega_f)}\cos((\omega_0+\omega_f)t+\phi)\right)$$

$$=-\frac{1}{2}\hat{r}p_0G_I\left(\frac{1}{(\omega_0-\omega_f)}\left\{\sin((2\omega_f-\omega_0)t-\phi)+\sin(\omega_0 t+\phi)\right\}+\frac{1}{(\omega_0+\omega_f)}\left\{\sin(-(\omega_0 t+\phi))+\sin((2\omega_f+\omega_0)t+\phi)\right\}\right)$$

$$=-\frac{1}{2}\hat{r}p_0G_I\left(\frac{1}{(\omega_0-\omega_f)}\sin((2\omega_f-\omega_0)t-\phi)+\frac{2\omega_f}{\omega_0^2-\omega_f^2}\sin(\omega t+\phi)+\frac{1}{(\omega_0+\omega_f)}\sin((2\omega_f+\omega_0)t+\phi)\right) \qquad (67)$$

Taking only the frequency ω_0 from (67) indicates the solution of the describing function.

$$y=-p_0G_I\frac{\omega_f}{\omega_0{}^2-\omega_f^2}\hat{r}\sin(\omega_0 t+\varphi)$$

Appendix E

The system is written in its differential equations.

$$\dot{v} = \frac{1}{Jc}\left(B(t)\lambda - \eta_A p_0 \sin(\omega_f t)\right)$$
$$\dot{x}_1 = K_{BPF} v - 2a x_1 - a^2 x_2$$
$$\dot{x}_2 = x_1$$
$$\dot{\lambda} = A(t) x_1$$

with $A(t) = 2G_1 \cos(\omega_f t)$, $B(t) = H_f \eta_f p_0 \sin(\omega_f t)$

Transformation to one state is:

$$\dot{\lambda} = A(t) x_1$$
$$\ddot{\lambda} = \dot{A}(t) x_1 + A(t)\dot{x}_1 = \dot{A}(t)\frac{\dot{\lambda}}{A(t)} + A(t)\dot{x}_1$$
$$\left.\begin{aligned}\dot{x}_1 &= K_{BPF} v - 2a x_1 - a^2 x_2\end{aligned}\right\}$$
$$\Rightarrow \ddot{\lambda} = \dot{A}(t)\frac{\dot{\lambda}}{A(t)} + A(t)\left(K_{BPF} v - 2a x_1 - a^2 x_2\right)$$
$$\ddot{\lambda} = \dot{A}(t)\frac{\dot{\lambda}}{A(t)} - 2a\frac{\dot{\lambda}}{A(t)} + A(t)K_{BPF} v - A(t)a^2 x_2$$
$$\dddot{\lambda} = \frac{d}{dt}\left(\frac{\dot{A}(t) - 2a}{A(t)}\right)\dot{\lambda} + \left(\frac{\dot{A}(t) - 2a}{A(t)}\right)\ddot{\lambda} + \dot{A}(t)K_{BPF} v + A(t)K_{BPF}\dot{v} - \dot{A}(t)a^2 x_2 - A(t)a^2 \dot{x}_2$$
$$\left.\begin{aligned}K_{BPF} v - a^2 x_2 &= \left(\dot{x}_1 + 2a x_1\right)\\ \dot{v} &= \frac{1}{Jc}\left(B(t)\lambda - \eta_A p_0 \sin(\omega_f t)\right)\\ \dot{x}_2 &= x_1\end{aligned}\right\}$$
$$\Rightarrow \dddot{\lambda} = \frac{d}{dt}\left(\frac{\dot{A}(t) - 2a}{A(t)}\right)\dot{\lambda} + \left(\frac{\dot{A}(t) - 2a}{A(t)}\right)\ddot{\lambda} + \dot{A}(t)\left(\dot{x}_1 + 2a x_1\right) + \frac{A(t)K_{BPF}}{Jc}\left(B(t)\lambda - \eta_A p_0 \sin(\omega_f t)\right) - A(t)a^2 x_1$$
$$\left.\begin{aligned}x_1 &= \frac{\dot{\lambda}}{A(t)}\end{aligned}\right\}$$
$$\Rightarrow \dddot{\lambda} = \frac{d}{dt}\left(\frac{\dot{A}(t) - 2a}{A(t)}\right)\dot{\lambda} + \left(\frac{\dot{A}(t) - 2a}{A(t)}\right)\ddot{\lambda} + \dot{A}(t)\left(\frac{d}{dt}\left(\frac{\dot{\lambda}}{A(t)}\right) + 2a\frac{\dot{\lambda}}{A(t)}\right) + \frac{A(t)K_{BPF}}{Jc}\left(B(t)\lambda - \eta_A p_0 \sin(\omega_f t)\right) - A(t)a^2\frac{\dot{\lambda}}{A(t)}$$
$$\dddot{\lambda} = \frac{d}{dt}\left(\frac{\dot{A}(t) - 2a}{A(t)}\right)\dot{\lambda} + \left(\frac{\dot{A}(t) - 2a}{A(t)}\right)\ddot{\lambda} + \dot{A}(t)\left(\frac{A(t)\ddot{\lambda} - \dot{A}(t)\dot{\lambda}}{A^2(t)}\right) + 2a\dot{A}(t)\frac{\dot{\lambda}}{A(t)} + \frac{A(t)K_{BPF}}{Jc}B(t)\lambda - \frac{A(t)K_{BPF}}{Jc}\eta_A p_0 \sin(\omega_f t) - a^2\dot{\lambda}$$
$$\Rightarrow \dddot{\lambda} + \left\{\left(\frac{\dot{A}(t) - 2a}{A(t)} + \frac{\dot{A}(t)A(t)}{A^2(t)}\right)\right\}\ddot{\lambda} + \left\{\frac{d}{dt}\left(\frac{\dot{A}(t) - 2a}{A(t)}\right) - \left(\frac{\dot{A}(t)}{A(t)}\right)^2 + 2a\frac{\dot{A}(t)}{A(t)} - a^2\right\}\dot{\lambda} + \left\{\frac{A(t)B(t)K_{BPF}}{Jc}\right\}\lambda = \frac{A(t)K_{BPF}}{Jc}\eta_A p_0 \sin(\omega_f t) \qquad (68)$$
$$\Rightarrow \dddot{\lambda} + \alpha_1\ddot{\lambda} + \alpha_2\dot{\lambda} + \alpha_3\lambda = f(t)$$

This system is written into its state-space description

$$\dot{\mathbf{x}} = C_\alpha(t)\mathbf{x} + \mathbf{e_n} f(t)$$

Here:

$$C_\alpha(t) = \begin{bmatrix} I^+_{n-1} & \mathbf{e}_{n-1} \\ -\boldsymbol{\alpha}^T & -\alpha_1 \end{bmatrix}$$
$$I^+_{n-1} = \begin{bmatrix} 0 & 1 & & 0 \\ & \ddots & \ddots & \\ & & \ddots & 1 \\ 0 & & & 0 \end{bmatrix}$$
$$\boldsymbol{\alpha}^T = [\alpha_n, \alpha_{n-1} \ldots \alpha_2]$$
$$\mathbf{e}_n^T = [0 \ldots 0,1]$$
$$\mathbf{x}^T = [x_1 \ldots x_n]$$

If there is a solution $\boldsymbol{p}^T$ for every α_n (with n = 3,2,1), the method of [7] can be used:

$$\dot{\mathbf{p}}^\mathbf{T} = -\mathbf{p}^\mathbf{T}\mathbf{e}_{n-1}\mathbf{p}^\mathbf{T} - \dot{\mathbf{p}}^\mathbf{T} I^+_{n-1} - \alpha_{4-n}\mathbf{p}^\mathbf{T} - \boldsymbol{\alpha}^\mathbf{T}$$